though Fig. 1 shows only those frequencies below 350 Hz, the spectrum was investigated to about 50 kHz. We were unable to find anything unusual in other than the region shown.

The displaced line implies motion at a preferred frequency, and our evidence indicates that this motion is ultimately connected with the active transport mechanism. It does not necessarily imply a preferred "pump frequency," however, since the deformational modes of the cells would tend to be excited even by a nonfrequency-selective mechanism.

A more comprehensive description of the experimental results and their theoretical interpretation is in preparation.

With pleasure we acknowledge helpful discussions with Dr. K. Green of the Wilmer Institute of The Johns Hopkins Medical Institutions, who also permitted us the use of his laboratory space to prepare the samples.

*Work supported in part by the U. S. Public Health Service under Research Grant No. NS 07226 from the National Institute of Neurological Diseases and Stroke.

†Presently with Middlesex Hospital Medical School, London, England.

[1]H. Z. Cummins and H. L. Swinney, in *Progress in Optics*, edited by E. Wolf (North-Holland, Amsterdam, 1970), Vol. VIII, p. 135.

[2]G. B. Benedek, in *Polarisation, Matière et Rayonnement, Livre de Jubilé l'honneur du Professeur A. Kastler*, edited by the French Physical Society (Presses Universitaire de France, Paris, France, 1969), p. 49.

[3]S. B. Dubin, J. H. Lunacek, and G. B. Benedek, Proc. Nat. Acad. Sci. 57, 1164 (1967).

[4]H. Z. Cummins, F. D. Carlson, T. J. Herbert, and G. Woods, Biophys. J. 9, 518 (1969).

[5]D. W. Schaefer, G. B. Benedek, P. Schofield, and E. Bradford, J. Chem. Phys. 55, 3884 (1971).

[6]N. C. Ford, W. Lee, and F. E. Karasz, J. Chem. Phys. 50, 3098 (1969).

[7]T. J. Herbert and F. D. Carlson, Biopolymers 10, 2231 (1971).

[8]Y. Yeh and R. N. Keeler, J. Chem. Phys. 51, 1120 (1969).

[9]Y. Yeh, J. Chem. Phys. 52, 6218 (1970).

[10]N. C. Ford and G. B. Benedek, Phys. Rev. Lett. 15, 649 (1965).

[11]H. L. Swinney and H. Z. Cummins, Phys. Rev. 171, 152 (1968).

[12]P. Bergé, B. Volochine, R. Billard, and A. Hamelin, C. R. Acad. Sci., Ser. B 265, 889 (1967).

[13]R. Nossal, S.-H. Chen, C.-C. Lai, Opt. Commun. 4, 35 (1971).

[14]F. B. Straub, Acta Physiol. Acad. Sci. Hung. 4, 235 (1953).

[15]G. Bardos and F. B. Straub, Acta Physiol. Acad. Sci. Hung. 12, 1 (1956).

[16]J. F. Hoffman, Circulation 26, 1201 (1962), and J. Gen. Physiol. 45, 837 (1962).

[17]H. Passow, in *The Red Blood Cell*, edited by C. W. Bishop and D. M. Surgenor (Academic, New York, 1964).

[18]H. A. Krebs, Biochim. Biophys. Acta 4, 249 (1950).

[19]It might be added at this point that hemolyzing the red blood cells in hypotonic Krebs bicarbonate Ringer solution (no ATP) resulted in ghosts which yielded a spectrum very similar to that with the inhibitor present in Fig. 1. Also red blood cells from a red cell pack resulted in this type of spectrum.

Observation of Neoclassical, Intermediate, and Pfirsch-Schlüter Diffusion in the dc Octopole*

Tihiro Ohkawa, John R. Gilleland, and Teruo Tamano
Gulf General Atomic Company, San Diego, California 92112
(Received 10 March 1972)

We have studied the plasma transport processes in the dc octopole with a toroidal magnetic field. The plasma diffusion is characterized by three principal collision-frequency regimes. The magnitude of the diffusion coefficient shows an inverse-square dependence on the magnetic field in all regimes. In the high-collision-frequency regime, the measured local diffusion coefficient agrees with Pfirsch-Schlüter diffusion in both rotational transform dependence and magnitude. Both for intermediate and low values of collision frequency, the enhancement of the decay rate agrees with neoclassical theory.

In this paper we shall describe the collisional transport observed in the dc octopole with a toroidal magnetic field. For an account of the transport with a pure octopole field, the reader is referred to previous publications.[1,2] These acticles also present the details of the construction and operation of the device. We remind the reader that the dc octopole with a toroidal magnetic field is an axisymmetric system with a major radius of 1.4 m. The octopole field is gen-

erated by six current rings, four of which are internal to the plasma. The toroidal field is produced by a 36-turn toroidal coil constructed external to the vacuum tank. The poloidal and toroidal fields are independently adjustable. In the measurements reported here, both fields are on the order of 100 G. At these fields, diffusion processes are predominant. Other losses, such as support losses and losses from recombination, are insignificant.

The plasma used in these studies is a hydrogen plasma injected from a coaxial gun. The initial density is 2×10^{11} cm^{-3}. An influx of neutral hydrogen gas from the gun causes the pressure in the tank to rise from about 1×10^{-7} Torr to 1×10^{-5} Torr in 100 msec. The diagnostics are Langmuir probes and a 3-cm microwave interferometer for density measurements, and an optical monochrometer for electron temperature measurements.

In the current series of measurements, the basic experimental plan is (1) to observe the plasma decay over a broad range of collision frequencies, (2) to determine the dependence of the decay rate upon the magnetic field strength and configuration, and (3) to calculate the experimental value of the local diffusion coefficient from detailed measurements of plasma density profiles and decay rates. The experimental results for the plasma decay are typified by Fig. 1. Here instantaneous density decay rate $1/\tau$ is plotted as a function of R_0/Λ, where R_0 is the major radius of the device and Λ is the mean free path for electron-ion momentum transfer. The figure is based upon the decay of the Langmuir probe current during a single plasma shot. Only the "late" decay is portrayed, when the electron temperature is constant at about 0.1 eV. One sees from Fig. 1 that the decay is always smooth, with no apparent instabilities. Further, it appears that the decay is characterized by three main regimes. In the high-collision-frequency regime the reciprocal of the density n is a linear function of t. This mode of decay continues until Λ becomes comparable to the machine dimension and the decay becomes approximately exponential. After further decay (large Λ), $1/n$ again becomes a linear function of t.

The dependence of the decay rate upon the magnetic field strength is shown in Fig. 2. Here the ratio of the poloidal field to the toroidal field was held constant and the reciprocals of plasma density are plotted as a function of t/B^2, where B is the total magnetic field. With this normalized time axis, almost exactly the same curves are observed for several different magnetic field strengths, although only two cases are shown in Fig. 2. Thus an inverse-square dependence of the plasma decay rate upon magnetic field strength is shown in all the regimes of decay.

The magnitude of the diffusion coefficient and its dependence upon rotational transform ι were determined as follows: In the high-collision-frequency regime, $n\tau$ profiles were measured for several different ratios of poloidal to toroidal current. Since in this regime $1/n$ is a linear function of t for all points in the profile, the shape of the profile is constant in time and $\partial(n\tau)/\partial t = 0$. Thus one may rewrite the diffusion equa-

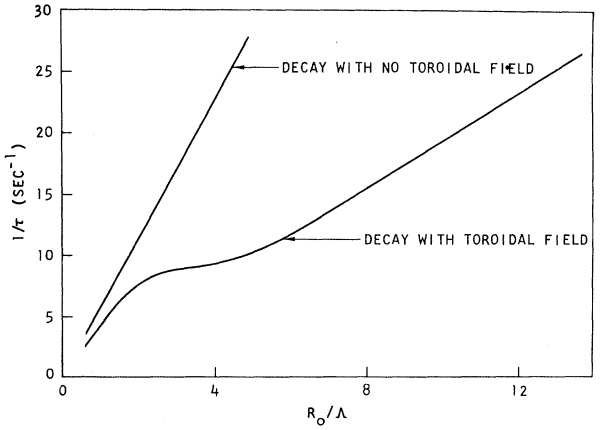

FIG. 1. Observed instantaneous decay rate plotted as a function of R_0/Λ. Lower curve, behavior in the combined toroidal and poloidal fields; upper curve, result with poloidal field only.

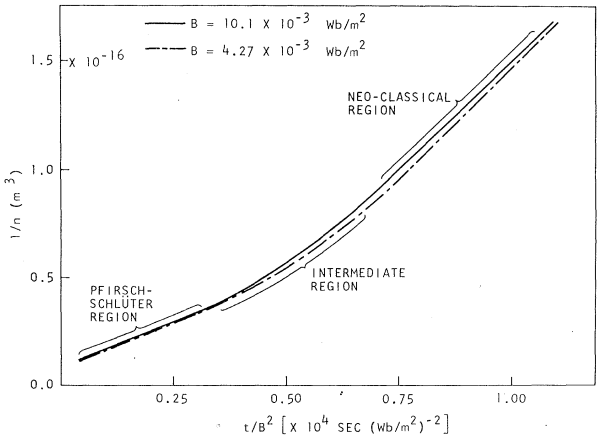

FIG. 2. Reciprocals of plasma density plotted as a function of t/B^2 for the different magnetic field strengths. Here the difference in B^2 is approximately 6.

tion as

$$\frac{\oint (D/2n)R^2 d\chi}{\oint R^2 d\chi/B^2} = \frac{\int_{\Psi_s}^{\Psi}[(n\tau)\oint d\chi/B_\chi{}^2]\,d\Psi}{\oint (R^2 d\chi/B^2)\,\partial(n\tau)^2/\partial\Psi}. \quad (1)$$

Here D is the diffusion coefficient, n the density, B_χ the poloidal field strength, Ψ the flux function, Ψ_s the value of the flux function at the separatrix, χ the magnetic potential, and R the local value of the major radius. If the diffusion is Pfirsch-Schlüter diffusion, then the left-hand side of Eq. (1) is

$$\frac{\oint (D/2n)R^2 d\chi}{\oint R^2 d\chi/B^2} = \eta\frac{(T_e + T_i)}{2} F, \quad (2)$$

where η is the perpendicular electric resistivity of the plasma and F is the Pfirsch-Schlüter enhancement factor. The general formula for the geometric factor F is given by Johnson and von Goeler[3] as

$$F \equiv \frac{D}{D_{\text{classical}}} = 1 + \left[\oint \frac{d\chi}{B^2 B_\chi{}^2} - \frac{(\oint d\chi/B_\chi{}^2)^2}{\oint B^2 d\chi/B_\chi{}^2}\right] \times (\oint d\chi/B^2 B_\varphi{}^2)^{-1}, \quad (3)$$

where B_φ is the toroidal field. Here we have neglected the difference between the perpendicular and parallel resistivities.

The right-hand side of Eq. (1) is evaluated as a function of Ψ from the experimental $n\tau$ profile. If this value is then divided by the corresponding Pfirsch-Schlüter factor F, the resulting quotient is found to be constant for the greater portion of Ψ space, as shown in Fig. 3(a). Since both the magnetic field strength B and the rotational transform ι vary with Ψ, this result confirms that the measured diffusion coefficient has the B dependence and ι dependence predicted by Pfirsch-Schlüter theory.

Another check of the ι dependence of the diffusion coefficient is given in Fig. 3(b). Here the enhancement of the diffusion is measured for different ratios of poloidal to toroidal coil current. The ratio of the measured diffusion coefficient to the classical diffusion coefficient is plotted as a function of $(2\pi/\iota)^2$. For all cases ι is evaluated at the same position in space. The dashed line is the Pfirsch-Schlüter enhancement factor calculated from the Johnson and von Goeler formula[3] for geometries of the dc octopole. The experimental values are indicated by the points and are in good agreement with the theory.

The theoretical value for the diffusion coefficient may be calculated using Spitzer's formula for η with the assumption that $T_e = T_i$. The value of the experimental diffusion coefficient is about 50% greater than the theoretical value for a temperature of 0.1 eV. By not maintaining the distinction between perpendicular and parallel resistivities in our theoretical estimates, we introduce an error of less than 30% for the range of ι values used in this experiment. This is within experimental errors.

In the low-collision-frequency regime, the plot of $1/\tau$ versus R_0/Λ approximates a straight line through the origin. The slope of this line is 2.2 times greater than the slope of the straight line observed in the high-collision-frequency regime. This feature strongly suggests neoclassical diffusion.[4] The observed ratio of slopes agrees with neoclassical theory within experimental error. The theoretical estimate of the ratio was made by evaluating the Rutherford formula[5] for the dc octopole geometry.

The two transition values of R_0/Λ are also in agreement with the theory.[5] These are the values of R_0/Λ at the transition from the Pfirsch-Schlüter region to the plateau region and at the transition from the plateau region to the neoclassical region. The theoretical values were evaluated for the regions of highest density gradient.

The residual plasma loss at extremely low densities ($R_0/\Lambda < 0.25$) shows an exponential decay. The exponential decay is observed only when the electron-ion collision frequency becomes of the order of the electron-neutral elastic collision frequency. Furthermore, the decay time shows a B^2 field dependence. Thus the residual diffusion at extremely low density is due to elastic collisions between electrons and the neutral hydrogen gas.

In Fig. 1 we have also plotted the decay observed with no toroidal field. The poloidal field is the same as that used in the case with the toroidal field on. The decay is in marked contrast to that observed with the toroidal field. Only two regimes of decay are observed. These are a $1/t$ decay at high density (classical diffusion) and the low-density exponential decay due to electron-neutral scattering. Note that, consistent with theory, the diffusion is faster than when both fields are used.

All of the previous discussion has been based upon data taken late in time by means of Langmuir probes. Much earlier in time, however, the three decay regimes are also seen with the microwave interferometer. This is because the high initial temperature of the plasma causes the

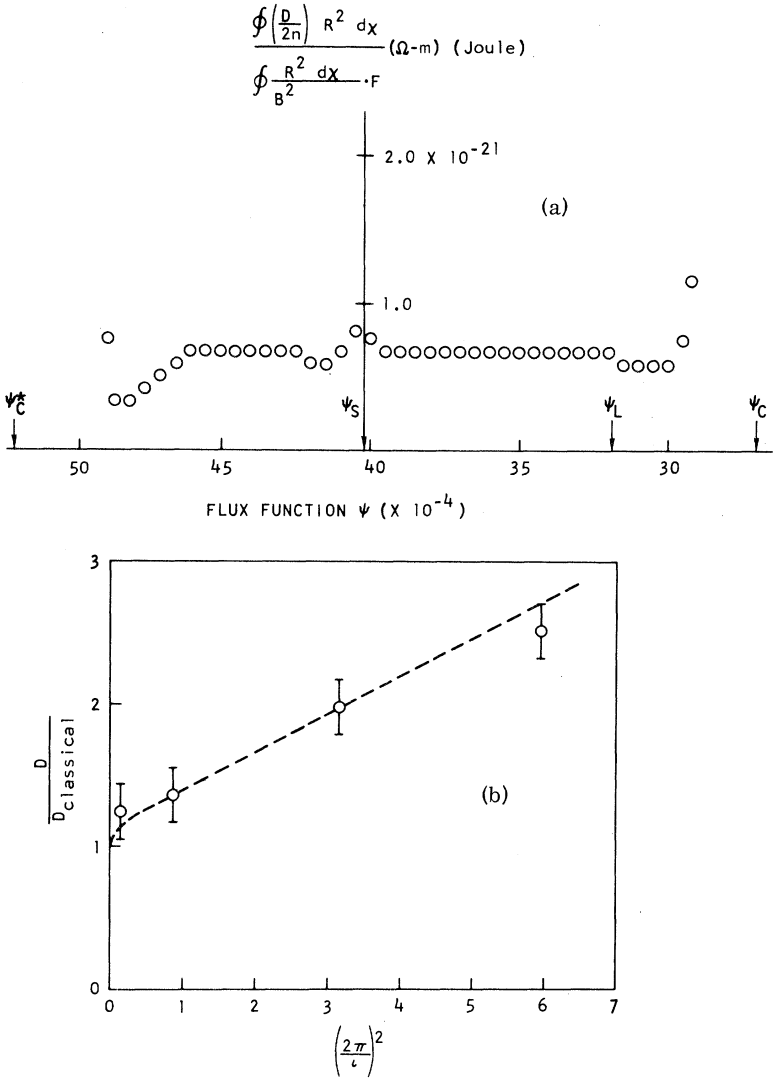

FIG. 3. (a) Values $\oint (D/2n) R^2 d\chi / [\oint (R^2/B^2) d\chi F]$, evaluated from the experimental $n\tau$ profile, plotted as a function of Ψ. (b) Ratio of measured diffusion coefficient to classical diffusion coefficient plotted as a function of $(2\pi/\iota)^2$, where ι is the rotational transform evaluated at a fixed point in space for various ratios of poloidal to toroidal coil current. Good agreement is obtained between the measured values (circles) and the calculated values from the formula by Johnson and von Goeler (dashed line).

collision frequency to be low, even though the density is high. The initial ion-neutral and electron-ion energy exchange times are both on the order of a few milliseconds and the plasma cools quickly. Since the mean free path depends upon the square of the temperature, it sweeps from the neoclassical to the classical range in about the first 10 msec. Curves very similar to Fig. 1 have been plotted from microwave data. The transition values of R_0/Λ agree within experimental error with those determined from the Langmuir probe data.

The results may be summarized as follows: Three major regimes of decay are observed. At high collision frequencies, $1/n$ is a linear function of t and the diffusion coefficient is proportional to n. Furthermore, the measured B dependence, ι dependence, and magnitude of the local diffusion coefficient agree with that predicted by Pfirsch-Schlüter theory. As the mean free path approaches a value on the order of the major radius, the decay becomes nearly exponential. For a mean free path greater than R_0, the diffusion coefficient again becomes proportional to n. The enhancement of the diffusion in this regime is consistent with the predictions of neo-

classical diffusion theory. Thus the experimental results are consistent with Pfirsch-Schlüter and neoclassical diffusion.

The authors wish to thank Dr. Dilip Bhadra for his help in the computer calculations.

*Work supported by the U. S. Atomic Energy Commission, Contract No. AT(04-3)-167.

[1]T. Ohkawa *et al.*, Phys. Rev. Lett. 24, 95 (1970).
[2]T. Ohkawa *et al.*, Phys. Rev. Lett. 27, 1179 (1971).
[3]J. L. Johnson and S. von Goeler, Phys. Fluids 12, 255 (1969).
[4]A. A. Galeev and R. Z. Sagdeev, Zh. Eksp. Teor. Fiz. 53, 348 (1967) [Sov. Phys. JETP 26, 233 (1968)].
[5]P. H. Rutherford, Phys. Fluids 13, 482 (1970).

Coherence Length in the Isotropic Phase of a Room-Temperature Nematic Liquid Crystal*

B. Chu, C. S. Bak, and F. L. Lin
Chemistry Department, State University of New York at Stony Brook, Stony Brook, New York 11790
(Received 11 February 1972)

The polarized ($I_{\parallel}$) and depolarized ($I_{\perp}$) scattered light intensity by fluctuations of the order parameter Q near the isotropic-nematic phase transition of para-methoxybenzylidene para-*n*-butylaniline has been measured as a function of the scattering angle over a range of temperatures above the phase-transition temperature T_p by means of two different incident wavelengths. Our results are in excellent agreement with the phenomenological theory of de Gennes. We also find the elastic constants $L_1 \gg L_2$ while L_1 depends upon temperature.

Potential applications of room-temperature nematic liquid crystals for electronic information display systems have stimulated the study of electrical properties and scattering behavior of para-methoxybenzylidene para-*n*-butylaniline (MBBA) which has an isotropic-nematic phase transition temperature T_p ranging from 41 – 47°C, depending upon impurities. Dielectric and resistivity anisotropy,[1,2] and anisotropic ultrasonic properties[3] of MBBA have been reported. Jones, Creagh, and Lu[4,5] have studied the dynamic scattering[6] characteristics of MBBA, while Litster and his co-workers have investigated the intensity and spectrum of scattered light in the nematic[7] as well as the isotropic phase.[8,9] However, Stinson,[8,10] Litster,[8,10] and Clark[10] failed to observe the angular anisotropy of scattered intensity for MBBA. In this Letter we report the results of an experimental study of the angular dependence of the intensity of light scattered by fluctuations of the order parameter[11] Q in the isotropic phase of MBBA.

For a system of rodlike molecules, the natural scalar order parameter S in a nematic phase is[12]

$$S = \tfrac{1}{2}\langle 3\cos^2\theta - 1\rangle , \tag{1}$$

where θ is the angle between the long axis of a molecule and the local nematic optic axis. It is, however, preferable to define the amount of order from a macroscopic property, independent of any assumption on the rigidity of the molecules. An appropriate order parameter may be taken as the anisotropic part of the dielectric tensor $\epsilon_{\alpha\beta}$,

$$Q_{\alpha\beta} = \epsilon_{\alpha\beta} - \tfrac{1}{3}\delta_{\alpha\beta}\epsilon_{\gamma\gamma} , \tag{2}$$

where α, β, and γ are the indices referring to the laboratory frame. $Q_{\alpha\beta}$ is a symmetric, traceless, second-rank tensor.

Near the isotropic-nematic phase transitions we assume that the free energy F per unit volume can be expanded in a Landau[13]-type power series in the order parameter,

$$F = F_0 + \tfrac{1}{2}AQ_{\alpha\beta}Q_{\beta\alpha} - \tfrac{1}{3}BQ_{\alpha\beta}Q_{\beta\gamma}Q_{\gamma\alpha} + O(Q^4) + \tfrac{1}{2}L_1(\partial_\alpha Q_{\beta\gamma})(\partial_\alpha Q_{\beta\gamma}) + \tfrac{1}{2}L_2(\partial_\alpha Q_{\alpha\gamma})(\partial_\beta Q_{\beta\gamma}) + \cdots , \tag{3}$$

where A and B are temperature-dependent coefficients, $\partial_\alpha = \partial/\partial\alpha$, L_1 and L_2 are the elastic constants in the isotropic phase, and repeated indices are summed. The coefficient A is expected to be small near the isotropic-nematic phase-transition temperature and has the form $A(T) = A_0\epsilon^{\gamma}$, with $\epsilon = (T - T^*)/T^*$, T^* being a temperature slightly below T_p, and γ a "critical" exponent. According to the mean field theory of Maier and Saupe, $\gamma = 1$.[12] Detailed discussions of these coefficients have been described else-